2001-1471

ROBUST FEEDBACK CONTROL OF A BAFFLED PLATE THROUGH VIBROACOUSTIC OPTIMIZATION

P. De Man*, A. François †and A. Preumont‡
Université Libre de Bruxelles, Active Structures Laboratory
CP. 165-42, 50 Av. F.D. Roosevelt, B-1050 Brussels, Belgium
e-mail: andre.preumont@ulb.ac.be

ABSTRACT

The active control of the noise radiation from a baffled plate is considered with a physical approach. A single input single output (SISO) control system is built by using a volume displacement sensor and a set of actuators (either point force or piezoceramics) driven in parallel by a single power amplifier. The actuators location is optimized to achieve an open-loop transfer function which exhibits the properties of a system with collocated actuator and sensor; the search procedure uses a genetic algorithm. The ability of a simple lead compensator to control this SISO system is numerically demonstrated.

1 INTRODUCTION

According to the modern control theory[1], an arbitrary control problem is mathematically formulated as the minimization of some norm of the closed-loop transfer function between the disturbance w and the performance metric z :

$$T_{zw} = G_{zw} + G_{zu}H(I - G_{yu}H)^{-1}G_{yw} \qquad (1)$$

where G_{zw} is the open-loop transfer function between the disturbance w and the performance metric z, G_{zu} between the control input u and the performance metric z, and G_{yw} between the disturbance w and the output measurement y, and G_{yu} between the control input u and the system output y. This abstract formulation, although mathematically attractive, does not explicitly take into account the particular features of the problem considered; in particular, for structural acoustics, the small stability margin of the plant, or its large modal density and large (in fact infinite) dimensionality.

For the problem considered in this study, the performance objective is to minimize the far field radiated noise power, which cannot be used directly for feedback and requires the application of radiation filters which reconstruct the radiated noise power from the modal information of the vibrating structure[2]. Radiation filters were first used in control design by Baumann et al.[3]; they were used in a LQG framework[4,5], and using H_∞ and $\mu-$synthesis[6]. Snyder et al.[7] used optimally shaped piezopolymer (PVDF) films to measure transformed modes in order to reconstruct structural radiation. At low frequency, the asymmetric modes with zero net volume velocity radiate poorly in the far field and the odd-odd modes are the dominant radiators; there is a strong correlation between the radiated sound power and the volume velocity (in fact, asymptotically, as $\omega \to 0$, the first radiation mode as defined by Cunefare[2] or by Elliott and Johnson[8] is proportional to the volume velocity). This brought the idea of developing volume velocity (or volume displacement) sensors which would allow to identify the single output measurement to the scalar performance metric. Identifying y and z in (1) brings substantial simplifications : $G_{zu} = G_{yu}$, $G_{zw} = G_{yw}$, and

$$T_{zw} = T_{yw} = (I - G_{yu}H)^{-1}G_{yw} \qquad (2)$$

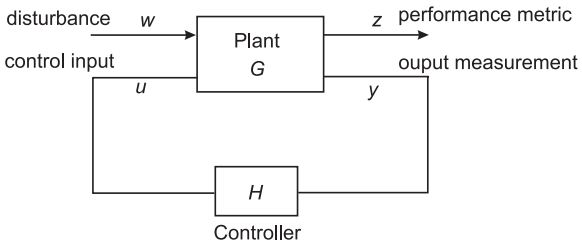

Figure 1: Block diagram of the control structure

*PhD student
†PhD student
‡Professor, Member AIAA

with the additional benefit of dealing with a single output (SO) system. Various volume velocity or displacement sensors have been proposed.[9,10,11] The one used in this study will be briefly described in section 3. Volume velocity sensors do not need additional filters.

For lightly damped vibrating structures, the open-loop system plays a role far more important than Equ.(2) suggests and the structure of G_{yu} depends critically on the type and location of the actuators and sensors. In particular, it is widely known that collocated actuator/sensor pairs are highly advisable whenever possible. Collocated point force actuator and velocity sensors have dissipative properties when used in a constant gain output feedback.[12,13] Even when they are not used in conjunction with purely dissipative controller the use of collocated actuator/sensor pairs brings some desirable robustness properties, and this may explain the quality of the results obtained by Cox et al.[6] with sensoriactuators. For lightly damped SISO systems, collocated actuator/sensor pairs guarantee alternating poles and zeros, and it is this key property which is responsible for the robustness of the control system.[14]

On the contrary to most papers devoted to this subject, this paper is concerned with the design of the *open-loop* system and attempts to devise a system with minimum complexity which is (i) easy to control (with a simple control law, possibly implemented in an analog manner), (ii) economical to implement (a single power amplifier) and (iii) robust to the parametric uncertainty (such as, for example, a shift in a natural frequency of the plate).

The paper is organized as follows : section 2 summarizes the control strategy; section 3 describes briefly the array sensor for the volume displacement (velocity); section 4 explains the optimization strategy to select the actuators location; a numerical example is treated in section 5 with point force actuators and piezoceramic patches. For illustration purposes, a simple feedback control law is numerically tested in section 6.

2 CONTROL STRATEGY

The objective of this study is to reduce the open-loop system (G_{yu}) to a SISO control problem with a number of desirable features from the point of view of controllability and robustness. The strategy uses a volume displacement sensor (see section 3) to reduce the problem to a single output problem. Next, a small set of actuators (either point force or piezoceramics) is constrained to operate with the same voltage to achieve a single input system, and the location of the actuators is optimized

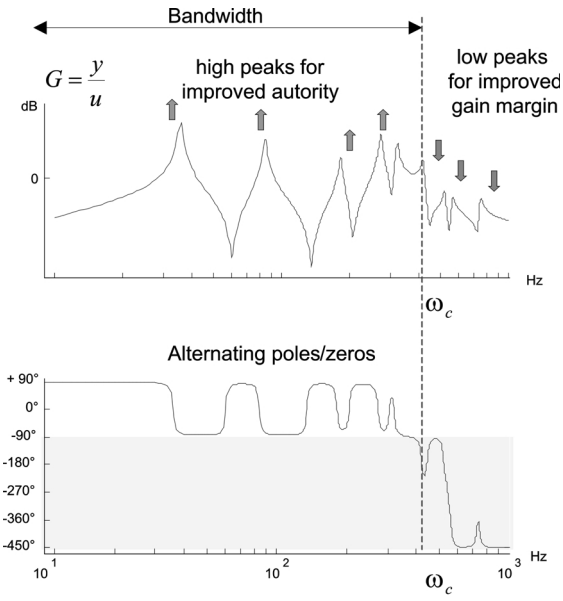

Figure 2: Desired features of the open-loop FRF

to provide the open-loop frequency response function (FRF) with the following desirable features illustrated in Fig.2 :

- Alternating poles and zeros are sought within the control bandwidth to enhance the immunity with respect to the parametric uncertainty.
- The magnitude of the resonance peaks is maximized within the control bandwidth to increase the control authority.
- The magnitude of the resonance peaks is minimized near and right after the cross-over frequency to improve the gain margin and reduce spillover.

The actuator placement optimization uses a genetic algorithm. The key in developing efficient genetic algorithms is to select a fitness function which, at the same time, matches the physical objectives and is easy to calculate. This is discussed in section 4.

3 VOLUME DISPLACEMENT SENSOR

The volume displacement sensor consists of an array of piezoelectric patches located at a regular mesh on the rectangular plate, connected to a linear combiner (Fig. 3), the coefficients of which are determined from experimental data (obtained from a laser scanner vibrometer) to supply the volume displacement.[11,15] This configuration is likely

to be superior to the previously proposed configurations based on shaped PVDF films[9,10], because it is less sensitive to local material properties and to manufacturing errors. The linear combiner is materialized by multiplying digital-to-analog converter (MDAC) components. The FRF reconstructed with the volume displacement sensor are in good agreement with measured ones, and the linear combiner coefficients are to a large extent independent of the disturbance source used in the experiment.[15]

This volume displacement sensor is now used as single output sensor (y) and performance metric (z).

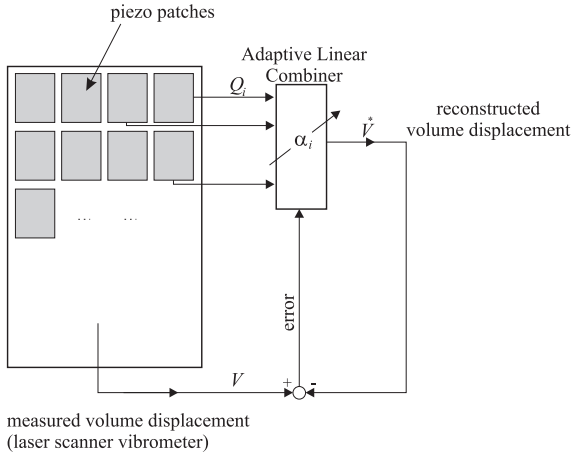

Figure 3: Principle of the volume displacement sensor for a rectangular plate

4 OPTIMIZATION OF THE ACTUATORS LOCATION

The optimization of the actuators location to achieve the features of the FRF described above is the main innovation of this paper. Our implementation of the genetic algorithm uses the MATLAB toolbox GAOT.[16] The challenge in this optimization problem is to formulate a fitness (cost) function which is easy to calculate and, at the same time, reflects the physical requirements of the open-loop FRF (Fig. 2). The modal expansion of the FRF between a single actuator and the volume displacement sensor takes the classical form

$$G(\omega) = \sum_{i=1}^{\infty} \frac{\phi_i(a) V_i}{\mu_i({\omega_i}^2 - \omega^2 + 2j\xi_i\omega\omega_i)} \qquad (3)$$

where μ_i, ω_i and ξ_i are the modal mass, the natural frequency and the modal damping of mode i, V_i is the modal volume displacement and $\phi_i(a)$ is the modal amplitude (displacement) at the actuator location. In case of several actuators acting in parallel with a single power source, $\phi_i(a)$ is simply the sum of modal amplitudes at the actuators location.

The alternating poles/zeros requirement can be expressed by using an interesting property of undamped SISO structural systems: *if two neighbouring modes are such that their residues have the same sign in the modal expansion of the open-loop FRF, there is always an imaginary zero between them.*[17] We thus define the following fitness function to be maximized :

$$F_1 = \sum_i sign[\phi_i(a) V_i] \qquad (4)$$

where $sign(.) = 1, 0, -1$ according to the sign of the argument. The sum over i extends to all the modes belonging to the frequency band where alternating poles and zeros are sought. Clearly, maximizing F_1 is equivalent to enforcing positive residues in the modal expansion (3).

Next, the good controllability of the modes within the bandwidth calls for a large modal amplitude at the actuator for all the modes within the controller bandwidth. This can be enforced by defining the second contribution to the fitness function :

$$F_2 = \sum_i \alpha_i |\phi_i(a)| \qquad (5)$$

where α_i are weighting factors. Finally, in order to minimize the controllability in the cross-over region and slightly beyond, the following contribution can be added :

$$F_3 = -\sum_j \beta_j |\phi_j(a)| \qquad (6)$$

this term is negative because the fitness function is maximized; β_i are also weighting factors. The global fitness function is

$$F = F_1 + F_2 + F_3 \qquad (7)$$

Notice that the above fitness function is straightforward to compute from the knowledge of the mode shapes only; this property is essential to speed up the optimization process. Note also that the limit between the modes contributing to the various contributions of the fitness function is flexible; some of the modes near crossover may be included in F_1 to guarantee alternating poles and zeros (in order to achieve phase stabilization), but also in F_3, to minimize their impact on the open-loop FRF.

5 APPLICATIONS

5.1 Point force actuators

The proposed strategy has been applied to the control of a 4mm thick glass plate of 1.28m x .58m. Table 1 lists the natural frequencies of the plate. The numerical study is performed with an analytical model of the plate, and we assume a perfect knowledge of the volume displacement output. Figure 4 shows the open-loop FRF for a single actuator arbitrarily located.

#1	*mode*	*Freq* Hz
1	(1, 1)	36 Hz
2	(1, 2)	54 Hz
3	(1, 3)	85 Hz
4	(2, 1)	125 Hz
5	(1, 4)	127 Hz
6	(2, 2)	143 Hz
7	(2, 3)	173 Hz
8	(1, 5)	182 Hz
9	(2, 4)	216 Hz
10	(1, 6)	249 Hz
11	(2, 5)	271 Hz
12	(3, 1)	273 Hz
13	(3, 2)	291 Hz
14	(3, 3)	322 Hz
15	(1, 7)	328 Hz
16	(2, 6)	338 Hz
17	(3, 4)	364 Hz
18	(2, 7)	417 Hz
19	(3, 5)	419 Hz
20	(1, 8)	420 Hz
21	(4, 1)	481 Hz
22	(3, 6)	486 Hz
23	(4, 2)	499 Hz
24	(2, 8)	508 Hz
25	(1, 9)	523 Hz
26	(4, 3)	529 Hz
27	(3, 7)	565 Hz
28	(4, 4)	572 Hz
29	(2, 9)	612 Hz
30	(4, 5)	627 Hz

Table 1: Natural frequencies of the plate

The frequency limit of the modes included in F_1 is chosen close to 250 Hz to include the first three modes contributing to the volume velocity (mode 1 at 36 Hz, 3 at 85 Hz and 8 at 182 Hz). Maximized controllability is required for modes 1,3 and 8 and minimized controllability is enforced for modes 12, 14, 15, 19, 25, and 27. Only the odd-odd modes are observable from the volume velocity sensor. The foregoing procedure has been applied for 1, 2 and 4 actuators working in parallel; Fig. 5 shows the open-loop FRF after optimization and the optimal actuator location. When using more than a single actuator a supplementary constraint has been added to the fitness function : as the analytical model provides mode shapes with a perfect symmetry, several solutions are possible for the same optimization problem. In order to avoid actuators located at the same place, we forced the actuator configuration to respect a certain symetry (i.e. in the case of 4 actuators, one actuator has been enforced in each quarter of the plate). The advantage of this constraint is that the modal participation of some unobservable modes is somewhat minimized, limiting by the same way control spillover. In every case, an alternating pole/zero configuration is easily obtained, but a larger number of actuators tends to improve the behaviour in the roll-off region, which eventually will allow larger gains.

An idea of the modal efficacy of the actuator configurations for the various modes can be obtained by computing the ratio

$$e_i = \frac{\sum_{j=1}^{n_a} \phi_i(j)}{n_a {\phi_i}^{max}} \tag{8}$$

where $\phi_i(j)$ is the amplitude of mode i at actuator j, n_a is the number of actuators working in parallel and ${\phi_i}^{max}$ is the maximum amplitude of mode i. The values of e_i for the optimal configurations are reported in Table 2. We indeed observe that the modal efficacy of the optimum actuator configurations is very small for the modes of which the controllability has been minimized (modes 12 to 27; mode 35 was purposely not included in this process).

mode	Hz	1 act.	2 act.	4 act.
1	36	0.33	0.37	0.40
3	85	0.80	0.73	0.70
8	182	0.80	0.44	0.33
12	273	0	0	0
14	322	0	0	0.02
15	328	0.33	0	0.02
19	419	0	0	0.02
25	523	0.33	0	0.02
27	565	0	0	0.02
35	748	0.33	0.33	0.15

Table 2: Modal efficacy e_i of the optimum point force actuator configurations

5.2 Piezoceramic actuators

The same problem has been addressed with piezoceramic actuators and the same set of modes

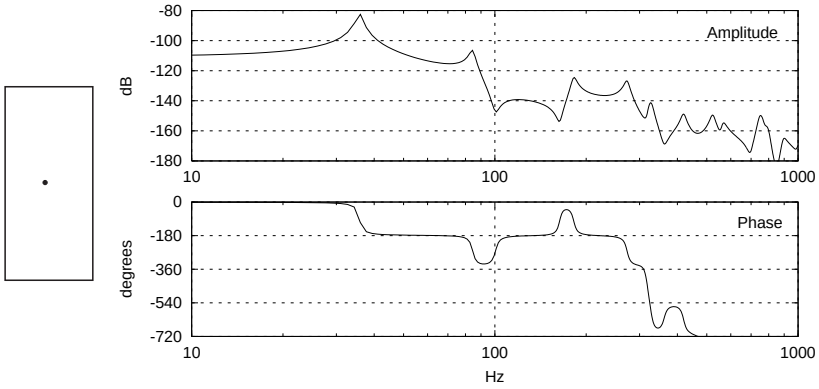

Figure 4: Open-loop FRF with arbitrary actuator location

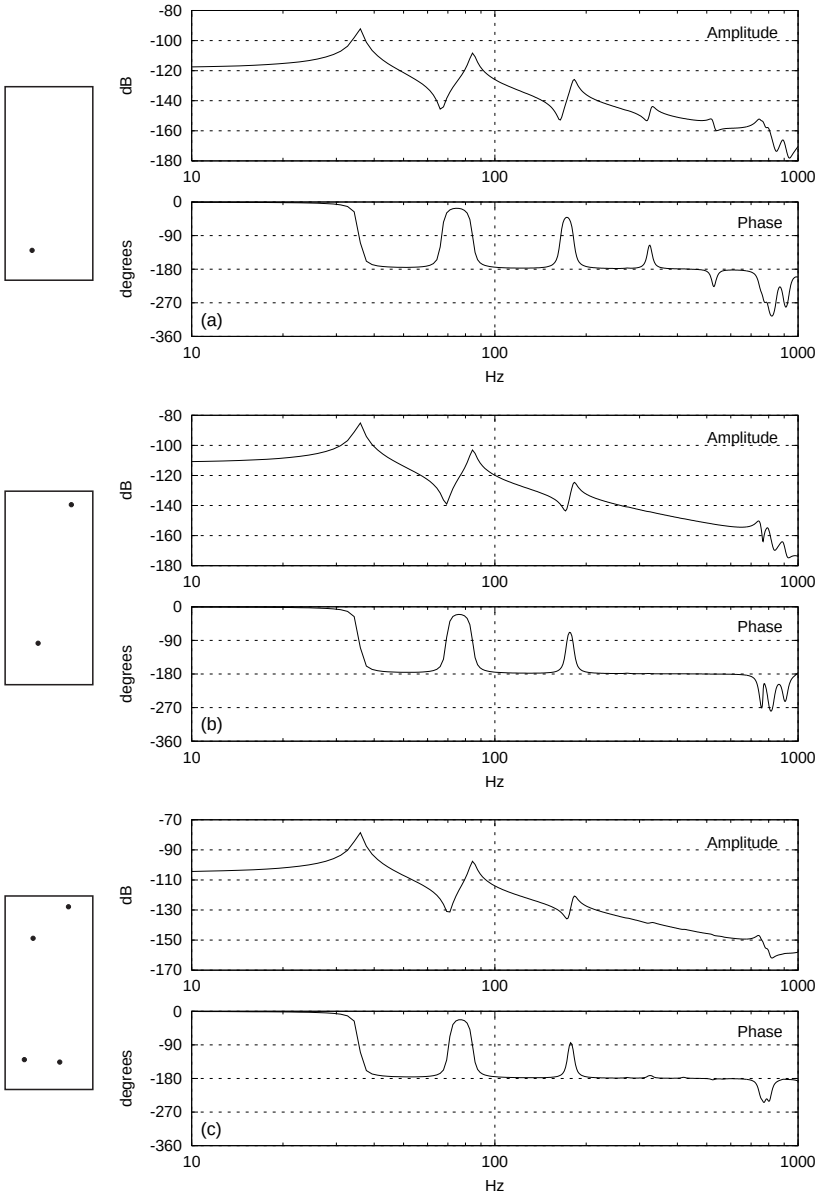

Figure 5: Open-loop FRF and optimum actuator locations for 1, 2 and 4 point force actuators

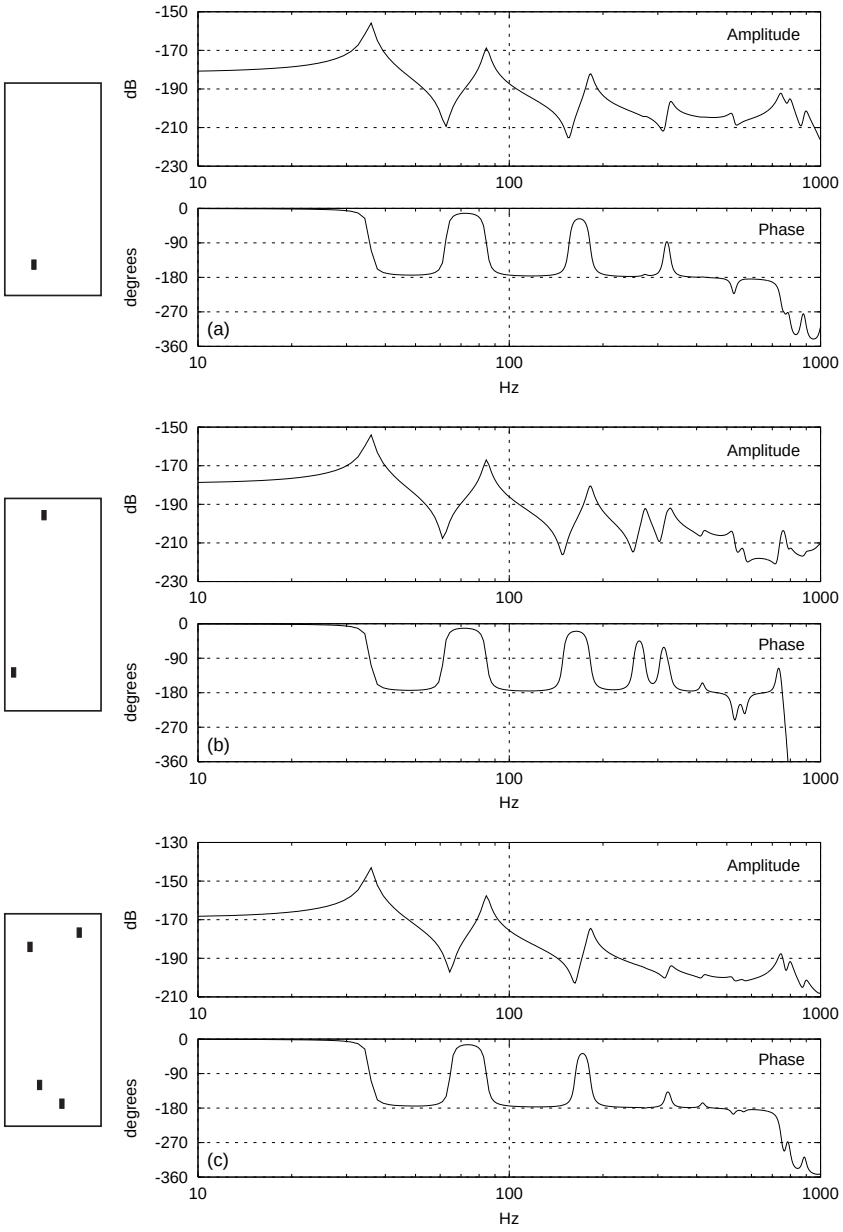

Figure 6: Open-loop FRF and optimum actuator locations for 1, 2 and 4 piezoceramic actuators

mode	Hz	1 act.	2 act.	4 act.
1	36	0.33	0.20	0.35
3	85	0.79	0.49	0.71
8	182	0.82	0.50	0.48
12	273	0	0.04	0
14	322	0	0.10	0.20
15	328	0.39	0.23	0.07
19	419	0	0.08	0.03
25	523	0.26	0.01	0.05
27	565	0	0.02	0.03
35	748	0.33	0.07	0.16

Table 3: Modal efficacy e_i of the optimum piezoceramic actuator configurations

have been selected to contribute to F_1, F_2 and F_3. The size of the piezo patch is 25 x 13.75 mm, and the orientation is fixed. Figure 6 show the open-loop FRF after optimization and the optimal locations for 1, 2 and 4 actuators (in this later case, an actuator has been enforced in every quarter of the plate). Alternating poles and zeros are obtained up to 500 Hz in all cases. We note that the strain actuator (piezo) tends to produce less roll-off above the optimization bandwidth; we will see next section how this reflects into the closed-loop performances. The values of e_i for the optimal configurations are reported in Table 3.

6 LOW AUTHORITY CONTROLLER

At this point, using a volume displacement sensor and the foregoing optimization strategy to locate the set of actuators working in parallel, we have achieved a "nice" SISO system with alternating poles and zeros and good controllability and reasonable roll-off at high frequency. This situation is typical of nearly collocated actuator/sensor configurations for which low-authority controllers work very well.[14] Although the benefit of our control strategy is not limited to low-authority controllers, we will illustrate it with a lead compensator, which is to a large extent insensitive to variations of the natural frequency of the structural modes within the control bandwidth (this is the prime source of uncertainty in vibration control). The three parameters g, T and α of the controller

$$H(s) = g\frac{Ts+1}{\alpha Ts+1} \qquad \alpha < 1 \qquad (9)$$

are determined as follows. T and α are chosen to provide a phase lead over the controlled bandwidth; the gain is determined to obtain a gain margin of no less than 10dB. The phase margin is 65 degrees. The FRF of the open-loop system consisting of the lead filter in series with the 4 point force actuators optimized configuration is shown Fig. 7.

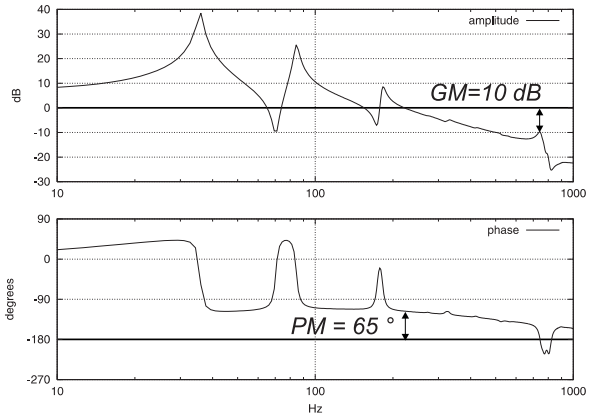

Figure 7: Open-loop FRF of the 4 point force actuators optimized configuration together with the lead filter

6.1 Point force actuators

The performance of the controlled system is evaluated with respect to a plane wave acoustical disturbance acting on part of the window in such a way as to excite all the modes. The FRF between the disturbance and the volume displacement, and the radiated sound power are compared in Fig.8 for the case of 4 point force actuators. The sound power is evaluated by discretizing the plate into elementary piston radiators.[8] As expected, the sound attenuation is limited to the modes participating to the volume displacement; some of the modes which do not contribute to the volume displacement do contribute to the sound power radiation; theses modes can be excited by the disturbance but also by the control force, depending on the actuator configurations. However, in Fig.8, we note very little spillover in the frequency band 500 Hz - 1000 Hz. Figure 9 shows the 1/3 - octave attenuation in dB. The foregoing results tend to confirm the good correlation between the attenuation of the volume displacement and the sound power radiation at low frequency.

6.2 Piezoceramics actuators

Figure 10 shows the same information as Figure 8 for an optimized configuration with 4 piezos. We note that piezoelectric actuators exhibit a stronger coupling to higher frequency modes. Figure 11 shows the 1/3 - octave attenuation in dB. The spillover above the controller bandwidth tends to

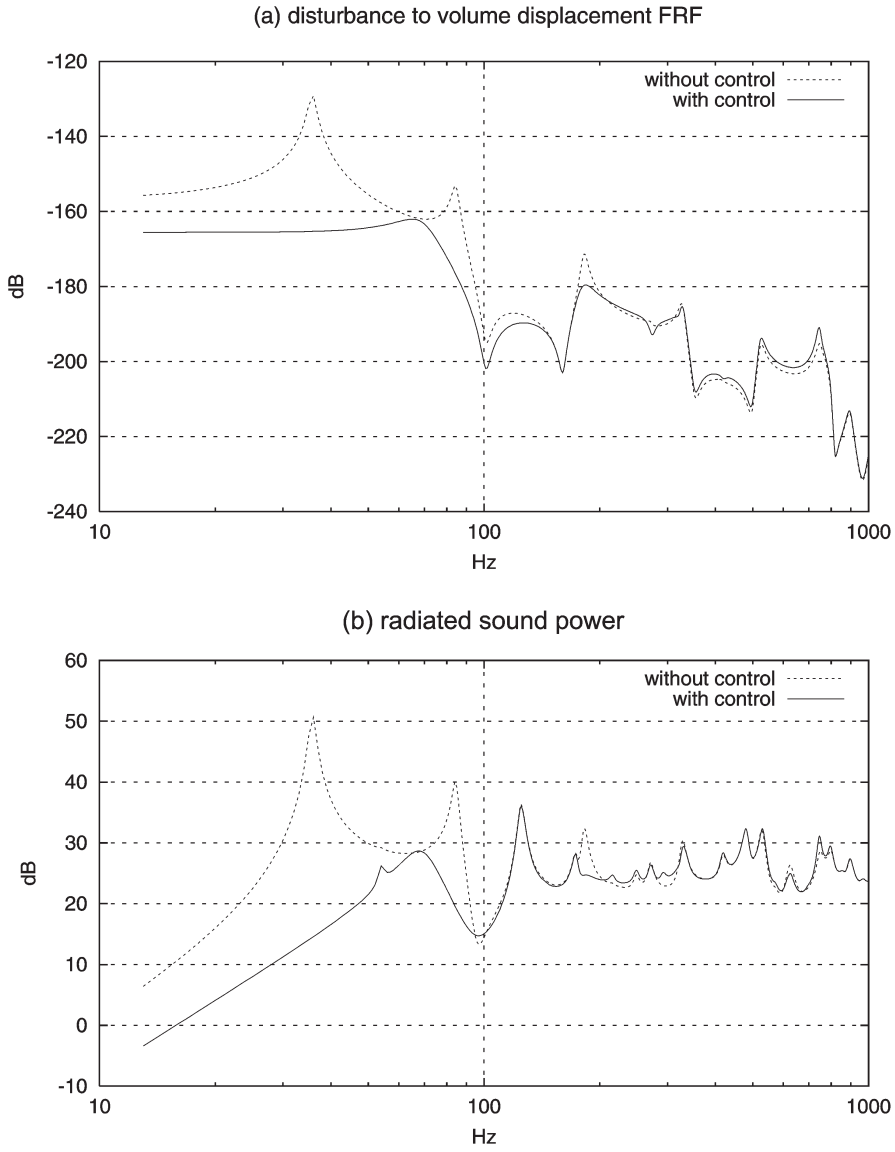

Figure 8: Effect of a lead compensator (4 point force actuators)

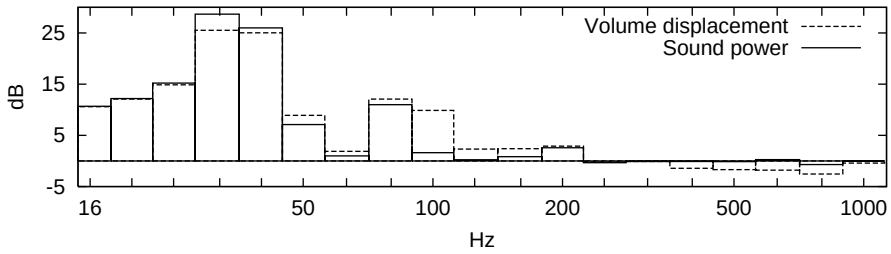

Figure 9: 1/3 - octave reduction (in dB). Point force actuators

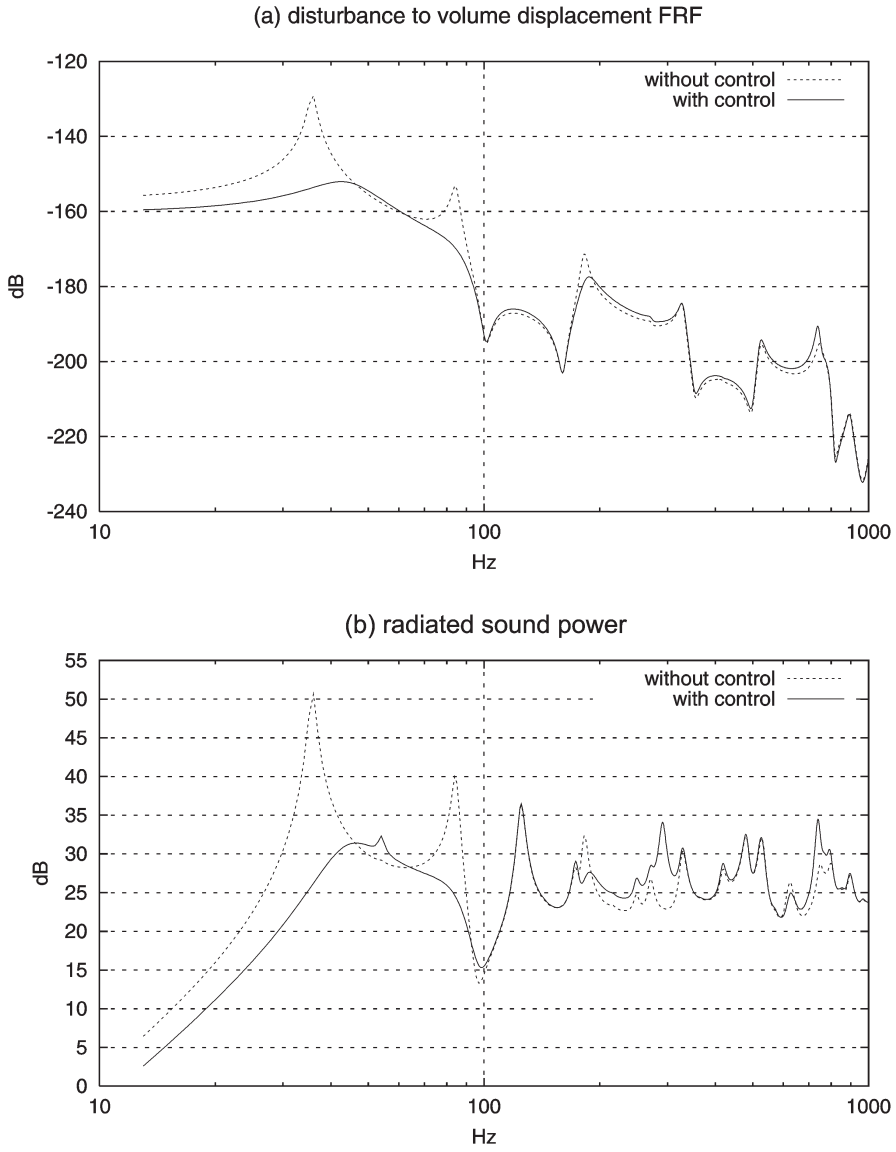

Figure 10: Effect of a lead compensator (4 piezoceramics actuators)

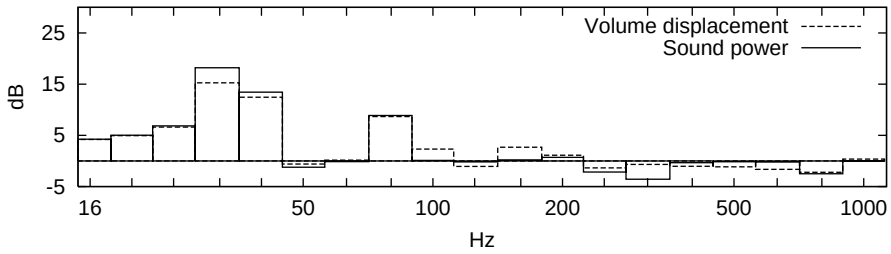

Figure 11: 1/3 - octave reduction (in dB). Piezoceramics actuators

		Frequency band					
		13-56 Hz		13-224 Hz		13-1120 Hz	
		Vol.	Power	Vol.	Power	Vol.	Power
pointe force	1	14.5	17	12	4.5	11.2	0.9
	2	18	21	14	7.5	12.9	2
	4	26	30	19	9	13.9	2.4
piezo patches	1	5	7	4	4	3.9	0.7
	2	8	10	7	5	5.6	1.1
	4	10.5	12.5	8.5	6	7.8	1.2

Table 4: Global attenuation of the volume displacement and sound power radiation (in dB) over various frequency bands for various actuator configurations.

be slightly higher with piezoceramics. Table 4 gives the global attenuation over various frequency bands for various actuator configurations. We see that the performances tend to be better with point force actuators than with piezoceramics and that they tend to improve with the number of actuators.

7 CONCLUSIONS

This paper has addressed the robust feedback control of a baffled plate from a new perspective which focuses on the open-loop system rather than on the controller design.

A SISO control has been built by using a volume displacement sensor and a set of actuators (either point forces or piezoceramics) driven in parallel by a single power amplifier. The actuator location is optimized to achieve some built-in robustness properties, namely alternating poles and zeros, and good controllability of the odd-odd modes within the control bandwidth, and reasonable roll-off at high frequency. The search procedure uses a genetic algorithm. The ability of a simple lead compensator to control the SISO system has been numerically demonstrated. More advanced controllers can also be used if necessary. An experiment is in preparation.

The optimization procedure for actuator location is the main innovation of this paper; we hope it will contribute to the design of cheaper, simpler and more robust control systems for vibroacoustic applications.

ACKNOWLEDGMENT

This work was supported by the Inter University Attraction Pole IUAP-IV-24 on Intelligent Mechatronics Systems and by the Ministry of *Région Wallonne* (DGTRE) under grants n°3512 and n°3363 (FIRST).

REFERENCES

[1] J.C. Doyle, B.A. Francis and R. Tannenbaum, *Feedback Control Theory*, Macmillan, 1992

[2] K.A. Cunefare, The minimum multimodal radiation efficiency of baffled finite beams, *J. Acoust. Soc. Am.*,Vol.90, No.5, pp.2521-2529, 1991

[3] W.T. Baumann, W.R. Saunders and H.R. Robertshaw, Active suppression of acoustic radiation from impulsively excited structures, *J. Acoust. Soc. Am.*, Vol.90, No.6, pp.3202-3208, 1991

[4] W. Dehandschutter, K. Henrioulle, J. Swevers, P. Sas, State-space feedback control of sound radiation using structural sensors and structural control inputs, *Proceedings ACTIVE 97*, Budapest, 21-23 August, pp.979-983, 1997

[5] J.S. Vipperman and R.L. Clark, Multivariable feedback active structural acoustic control using adaptive piezoelectric sensoriactuators, *J. Acoust. Soc. Am.*,Vol.105, No.1, pp.219-225, 1999

[6] D.E. Cox, G.P. Gibbs, R.L. Clark and J.S. Vipperman, Experimental robust control of structural acoustic radiation, *Journal of Vibration and Acoustics*,Vol.121, pp.433-439, 1999

[7] S.D. Snyder, N. Tanaka and Y. Kikushima, The use of optimally shaped piezo-electric film sensors in the active control of free field structural radiation, Part 2: feedback control, *Journal of Vibration and Acoustics*, Vol.118, pp.112-121, 1996

[8] S.J. Elliott and M.E. Johnson, Radiation modes and the active control of sound power, *J. Acoust. Soc. Am.*, Vol.94, No.4, pp.2194-2201, 1993

[9] J. Rex and S.J. Elliott, The QWSIS - a new sensor for structural radiation control. Proceedings of MOVIC, Yokohama, pp.339-343, September 1992

[10] F. Charette, A. Berry and C. Guigou, Active control of sound radiation from a plate using a polyvinylidene fluoride volume displacement sensor, *J. Acoust. Soc. Am.*, Vol.103, No.3, pp.1493-1503, 1997

[11] A. Preumont, A. François and S.Dubru, Piezoelectric array sensing for Real-Time, Broad-Band Sound Radiation Measurement, *Journal of Vibration and Acoustics*, Vol.121, pp.446-452, 1999

[12] G.C. Smith and R.L.Clark, The influence of frequency-shaped cost functionals on the structural acoustic control performance of static, output feedback control, *J. Acoust. Soc. Am*, Vol.104, No.4, pp.2236-2244, 1998

[13] R.L. Clark and D.E.Cox, Multi-variable structural acoustic control with static compensation, *J. Acoust. Soc. Am*, Vol.102, No.5, pp.2747-2756, 1997

[14] A. Preumont, *Vibration Control of Active Structures, An Introduction*, Kluwer, 1997

[15] A. François, P. De Man and A. Preumont, Piezoelectric array sensing of volume displacement: a hardware demonstration, to be published in the Journal of Sound and Vibration, 2001.

[16] C.R. Houck, J.A. Joines, M.G. Kay, A genetic Algorithm for Function Optimization : A Matlab Implementation, Technical Report 96-01, NCSU-IE, 1995

[17] G.D. Martin, On the control of flexible mechanical systems. Master's thesis, Stanford University, 1978